Distribution of squeezed states through an atmospheric channel

Christian Peuntinger,[1,2,*] Bettina Heim,[1,2,3,*] Christian R. Müller,[1,2]
Christian Gabriel,[1,2] Christoph Marquardt,[1,2,3] and Gerd Leuchs[1,2,3]

[1] *Max Planck Institute for the Science of Light, Günther-Scharowsky-Straße 1/Building 24, Erlangen, Germany*
[2] *Institute for Optics, Information and Photonics, University of Erlangen-Nuremberg (FAU), Staudtstraße 7/B2, Erlangen, Germany*
[3] *Erlangen Graduate School in Advanced Optical Technologies (SAOT), FAU*

(Dated: February 26, 2014)

Continuous variable quantum states of light are used in quantum information protocols and quantum metrology and known to degrade with loss and added noise. We were able to show the distribution of bright polarization squeezed quantum states of light through an urban free-space channel of 1.6 km length. To measure the squeezed states in this extreme environment, we utilize polarization encoding and a post-selection protocol that is taking into account classical side information stemming from the distribution of transmission values. The successful distribution of continuous variable squeezed states is accentuated by a quantum state tomography, allowing for determining the purity of the state.

PACS numbers: 03.67.Hk, 42.50.Dv, 42.68.Bz

arXiv:1402.6290v1 [quant-ph] 25 Feb 2014

INTRODUCTION

The survival of quantum states in hostile environments is of crucial importance in quantum information processing and of general interest in the understanding of decoherence processes. The transmission of quantum states of light through an atmospheric link is such a demanding task. Free-space quantum state distribution has the potential to form a key component in future quantum networks. It offers the possibility of distributing quantum states with high flexibility in the required infrastructure. Furthermore, links to moving objects, like vehicles, planes and satellites are conceivable. Recent experiments demonstrated free-space quantum channels in long range ground-to-ground links [1–6] as well as in a link from a ground station to a plane [7]. Other experiments study the feasibility of quantum communication between earth and space in general [8–14] or the effects of atmospheric turbulence on quantum states in particular and how to exploit them [15–17]. All these experiments (for a general review on free-space quantum communication experiments see [18]), are based on discrete variables (DV) i.e. rely on photon counting at the receiver. On the other hand recent investigations have proven the feasibility of continuous variable (CV) free-space quantum key distribution [19–21]. By using homodyne receivers, this approach can offer high speed detection and immunity to stray light. Squeezed states can be used in CV quantum key distribution protocols [22, 23] and it has been proven [24] that they can provide an enhancement compared to coherent states. When transmitting CV quantum states much care has to be taken to avoid their decoherence. Losses will result in a degradation of the quantum states whereas in DV systems these will merely lower the detection rate. Also, phase relations and waveform distortions play an important role as the applied homodyne detection relies on optical interference and a high homodyne efficiency is crucial. Thus the save transmission of CV quantum states in harsh environments poses a major challenge in different physical systems, ranging from optical free-space links to superconducting cavity quantum electrodynamics [25].

In this Letter we demonstrate the distribution of bright CV squeezed states of light through a turbulent atmospheric channel. The atmosphere introduces fluctuations in amplitude and phase. Due to the fluctuating phase and the resulting wave front distortions, standard homodyne measurements at the receiver are challenging. We circumvent this problem by using polarization encoding. Polarization offers a distinct advantage in this case. The different polarization components can be measured separately yet they occupy the same spatial mode and experience identical distortions. Measuring the polarization components averaged over the beam cross section is like a differential measurement, where the distortions cancel out. In that sense the polarization measurement is analogous to measuring in a decoherence free subspace [26, 27] and is immune to phase fluctuations. Bright polarization squeezed states are equivalent to combining a bright coherent polarization mode and an orthogonally polarized vacuum squeezed mode [28, 29]. Thus we are able to utilize polarization measurements, which can be approximated as homodyne measurements with a bright local oscillator and a polarization multiplexed squeezed vacuum signal. The system is inherently immune to stray light allowing for daylight operation without any further spectral or spatial filtering. CV polarization encoding perfectly fits atmospheric transmission systems [19, 20] and additionally the polarization of the light field is easy to manipulate without introducing considerable loss.

The atmospheric channel introduces fluctuations of the intensity through beam wandering, distortion and

spreading. Special care is necessary to take into account the resulting variation of the shot noise level during our measurements. We developed a post-selection protocol that is also able to enhance the degree of squeezing compared to that of the raw channel data. These results are substantiated by a quantum state reconstruction via a maximum likelihood algorithm [30–33].

CONCEPT OF OUR EXPERIMENT

Our experiment is based on a realistic free-space *channel* of 1.6 km length in the city of Erlangen (see FIG. 1a). The channel is located in a truly urban environment. The optical beam path starting from the sender *(Alice)* runs past buildings, heated rooftops, heavy traffic and forests. This inhomogeneous environment leads to significant turbulence affecting phase and intensity. The beam is received by *Bob*, located in the 12th floor of a university building. In the following paragraph, we explain the details of our setup consisting of a robust source of polarization squeezed states of light at *Alice*, and a detection stage at *Bob*.

At *Alice*, we generate CV polarization squeezed states in a compact and stable setup by exploiting the Kerr-nonlinearity of a single mode fiber [34, 35] (see FIG. 1b). The source is able to operate without any need of controlled laboratory conditions. All components are built onto a breadboard with an area less than $0.3\,\mathrm{m}^2$. A commercial soliton-laser (Origami, *Onefive GmbH*) emits femtosecond pulses (200 fs) at a center wavelength of $\lambda_0 = 1559\,\mathrm{nm}$ and a repetition rate of 80 MHz. Shorter wavelengths offer an enhanced collection efficiency after channel transmission at a given aperture size. Therefore, the sending and receiving optics of our free-space channel are optimized for wavelengths in the 800 nm range, which also coincides with low atmospheric losses. Consequently, we use a periodically poled lithium-niobate crystal (MSHG1550-0.5-0.3, *Covesion Ltd.*) to convert the output of the laser to its second harmonic at $\lambda_1 = 780\,\mathrm{nm}$, and dichroic mirrors for subsequent spectral filtering. For the preparation of the CV polarization squeezed states we use both axis of a birefringent polarization maintaining photonic crystal fiber (NL-PM-700, zero dispersion wavelength $\lambda_{ZD} = 700\,\mathrm{nm}$, *Crystal Fibre A/S*). Due to the nonlinear Kerr-effect in this fiber we individually quadrature squeeze two orthogonally polarized pulses. These two pulses are overlapped to produce a circularly polarized state, showing polarization squeezing. To achieve this we have to precompensate the birefringence of the fiber with different optical path lengths in front of the fiber. We actively control the overlap and the phase between the two pulses by tapping 0.1 % of the signal after the fiber and controlling a piezoelectric actuator used in an interferometer-like configuration before the fiber.

For the description of the state of polarization the Stokes operators [29] are used:

$$\begin{aligned}
\hat{S}_0 &= \hat{a}_{\mathrm{H}}^\dagger \hat{a}_{\mathrm{H}} + \hat{a}_{\mathrm{V}}^\dagger \hat{a}_{\mathrm{V}} \quad (\textit{total intensity}),\\
\hat{S}_1 &= \hat{a}_{\mathrm{H}}^\dagger \hat{a}_{\mathrm{H}} - \hat{a}_{\mathrm{V}}^\dagger \hat{a}_{\mathrm{V}} \quad (\textit{horizontal/vertical polarization}),\\
\hat{S}_2 &= \hat{a}_{\mathrm{H}}^\dagger \hat{a}_{\mathrm{V}} + \hat{a}_{\mathrm{V}}^\dagger \hat{a}_{\mathrm{H}} \quad (\pm 45^\circ\ \textit{polarization}),\ \text{and}\\
\hat{S}_3 &= \mathrm{i}(\hat{a}_{\mathrm{V}}^\dagger \hat{a}_{\mathrm{H}} - \hat{a}_{\mathrm{H}}^\dagger \hat{a}_{\mathrm{V}})(\textit{left/right handed polarization}),
\end{aligned}$$

with the field operators for the horizontally and vertically polarized mode $\hat{a}_{\mathrm{H,V}}$ and $\hat{a}_{\mathrm{H,V}}^\dagger$. In terms of these Stokes operators, our state has a mean value of zero for $\hat{S}_1$ and $\hat{S}_2$, while $\langle \hat{S}_3 \rangle \gg 0$. In Poincaré space the plane perpendicular to $\hat{S}_3$ is called dark plane in this case. The combined circularly polarized light pulses have a continuous wave equivalent optical power of 1.37 mW and show squeezing along one particular measurement direction within the S_1-S_2 dark plane, $S_{\theta_{sq}}$, and anti-squeezing in the orthogonal direction $S_{\theta_{sq}+90^\circ}$ [34]. A typical squeezing value measured at *Alice* with an electrical spectrum analyzer at a sideband-frequency of 12 MHz, a resolution bandwidth of 300 kHz, and a video bandwidth of 30 Hz is $-2.8 \pm 0.1\,\mathrm{dB}$. The high anti-squeezing value of $16.9 \pm 0.1\,\mathrm{dB}$ is a result of quantum noise and excess noise from photon-phonon interactions in the fiber. Finally, the optical beam is expanded by a telescope decreasing the divergence of the beam. The prepared states are distributed through the free-space *channel*.

At *Bob*, it is important to collect as much as possible of the incoming light field to minimize degrading loss. Simultaneously it is crucial to avoid any disturbance of the state of polarization. Therefore, we do not use a mirror but an achromatic lens with a diameter of 150 mm and a focal length of $f = 800\,\mathrm{mm}$ to collect the light. A half-wave plate (HWP) and a polarizing beamsplitter (PBS) are placed slightly before the focal point, such that the beam can directly be focused onto two pin-diode detectors behind the PBS (see FIG. 1c). The AC-outputs of these custom made detectors are mixed with a 12 MHz radio frequency local oscillator (arbitrary waveform generator 33250A, *Agilent Technologies Inc.*), amplified (wideband voltage amplifier DHPVA-100, *FEMTO Messtechnik GmbH*), low pass filtered (BLP-1.9, *Mini-Circuits Laboratory*, 3 dB cut off frequency 2.5 MHz) and digitized by an analoge-to-digital converter (AD-card, CompuScope CS1610, *GaGe a product brand of DynamicSignals LLC*) with a sampling rate of 10 MSamples/s. The bandwidth of the DC-outputs, that are sampled simultaneously with identical sampling rates, is 150 kHz, and thus sufficient for the atmospheric fluctuations. This setup allows us to measure the Stokes observables in the S_1-S_2 dark plane at a sideband frequency of 12 MHz with a bandwidth of 2.5 MHz (given by the used low pass filters) by calculating the difference of the two, still oversampled, AC signals. The measured Stokes observable within the S_1-S_2 dark plane can be choosen by rotating the HWP.

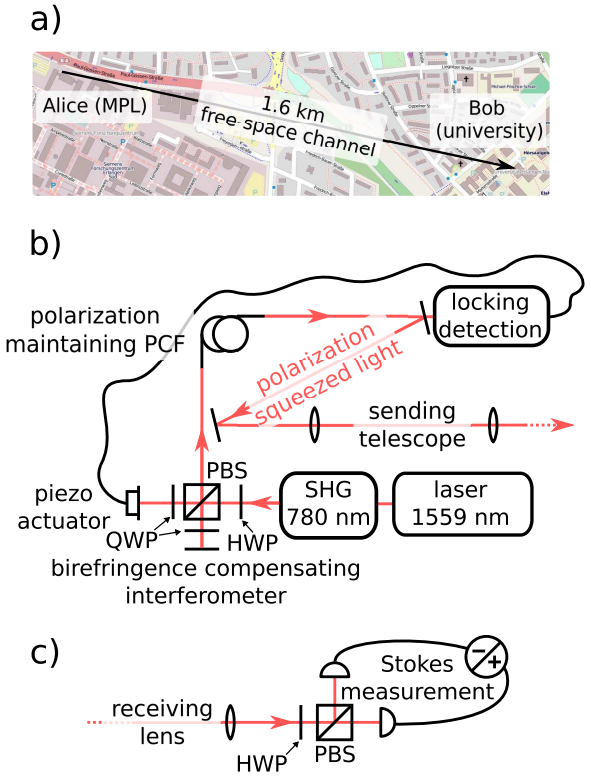

FIG. 1. Schematic drawing of the experimental setup. Used abbreviations: SHG, second harmonic generation; HWP, half-wave plate; QWP, quarter-wave plate; PBS, polarizing beam-splitter; PCF, photonic crystal fiber; a) A street map of our free-space channel. The sender *(Alice)*, located at the roof of the MPL institute's building, is connected by a 1.6 km atmospheric transmission line with the receiving station *(Bob)*, which is placed in a tall university building. b) The source of the bright polarization squeezed quantum states. c) At the receiver we directly focus onto two detectors after splitting the beam by a combination of a HWP and a PBS. The difference signal of these detectors corresponds to a Stokes observable within the S_1-S_2 dark plane, dependent on the orientation of the HWP.

The sum of the AC signals gives rise to the S_0-signal. The sum of the DC signals, from which we can calculate the respective transmission values, can be used as classical side information.

RESULTS

A turbulent atmosphere leads to beam wandering, distortion and spreading and thus to continuous fluctuations of the intensity at the receiver. This directly results in a varying shot noise level during our measurements. It is important to account for this with a proper shot noise calibration and monitoring. We use the transmission value obtained as classical side information and sort all collected data according to the prevailing transmission value into bins with a width of 0.19 % of the total optical power sent from *Alice* (corresponding to 2.6 μW). With this technique we are able to compare the measured Stokes parameter variance to the corresponding shot noise variance.

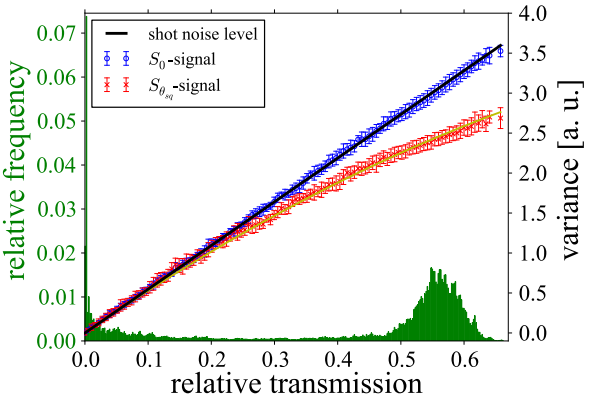

FIG. 2. Verification of transmitted squeezed states: Measurement of the polarization squeezed signal with additional artificially induced loss at the receiver. The S_0-signal, which determines the shot noise limit, scales linear with the transmission value (fitted in black). In good agreement to theory the polarization squeezed signal $S_{\theta_{sq}}$ scales quadratically with the transmission value (fitted in yellow). We show only every third data point for clarity. The green histogram shows the transmission statistics, which is a result of the natural fading channel and artificial attenuation.

A reliable way to prove genuine detection of squeezed states is to compare the attenuation of the quantum states with its theoretical prediction. Squeezed states show a distinct behaviour that can be discriminated from classical noise and rule out technical effects such as saturation of the detectors. We use both the natural fluctuation in transmission and additional attenuation of the beam imposed at the receiver to be able to measure the squeezed states at Bob for all transmission values down to zero (see FIG. 2). The additional attenuation was achieved by moving an optically dense material into the beam at the receiver stage. We average the variances of the total intensity and the $S_{\theta_{sq}}$ and $S_{\theta_{sq}+90^\circ}$ Stokes parameters over 10000 samples for each individual transmission bin and discard all bins containing less than 50000 samples. Thus, at least 5 variances and their mean value were obtained for each bin. To give a conservative estimate of the error of these measurements the error-bar indicates one standard deviation of the deduced variances. The S_0-signal (blue circles) scales linearly with the transmission (black fit), which is in perfect agreement to a shot noise limited signal. The polarization squeezed signal $\hat{S}_{\theta_{sq}}$ (red crosses) scales quadratically (yellow fit) as expected from theory [36] and is below the shot noise level. The normalized green histogram visualizes the transmission statistics during this measurement.

In FIG. 3 the measurement of the Stokes-observable $\hat{S}_{\theta_{sq}+90^\circ}$ (red crosses) in the S_1-S_2 dark plane is shown.

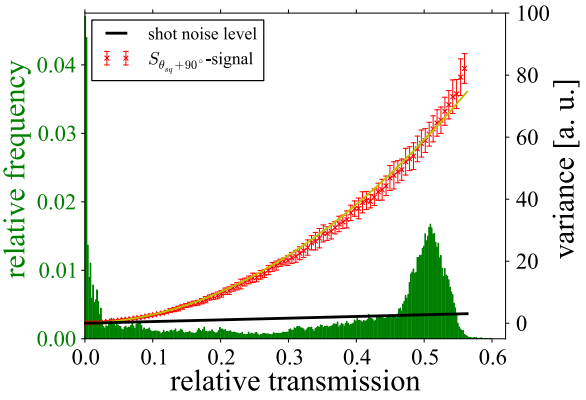

FIG. 3. Measurement of the polarization anti-squeezed signal with classical excess noise and additional artificially induced loss at the receiver. Note that the classical excess noise is very high due to the photon-phonon interaction in the fiber used at *Alice*. The signal scales quadratically (fitted in yellow) as expected from theory. We show only every third data point for clarity. The green histogram shows the transmission statistics for this measurement.

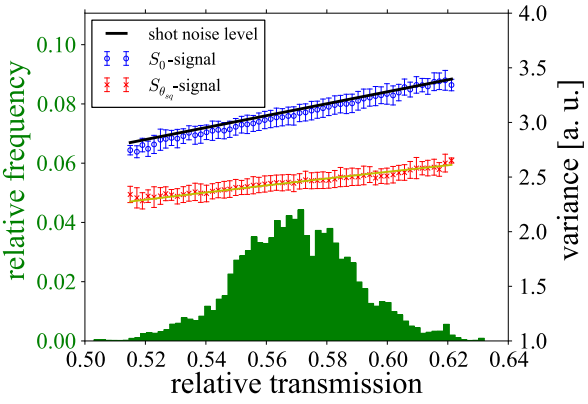

FIG. 4. Measurement of the polarization squeezed signal with natural transmission statistics of the free-space channel. The green normalized histogram shows the transmission statistics. With the state selection protocol we can improve the squeezing value from $-0.95\,\mathrm{dB}$ to $-1.08\,\mathrm{dB}$ relative to shot noise variance.

This observable shows anti-squeezing as well as classical excess noise stemming mostly from photon-phonon interaction in the fiber used for squeezed light generation in the sender setup. The variance also scales quadratically with the transmission value (fitted in yellow), while the black line indicates the shot noise limit as given by the fitted curve of FIG. 2.

After verifying the genuine transmission of squeezed states we investigated the natural transmission statistics of our free-space fading channel. The transmission statistics is shown in FIG. 4 as a normalized green histogram. The squeezing value for the squeezed state with the highest transmission value is $-1.08 \pm 0.04\,\mathrm{dB}$ below the shot noise variance, slightly increased compared to the average amount of squeezing of $-0.95 \pm 0.03\,\mathrm{dB}$. The enhancement by the post-selection protocol depends on several parameters. This will be more pronounced if the investigated channel transmission covers a broader range or if the highest possible channel transmission would be closer to the physical limit of 1. Finally this post-selection technique becomes most important if the initial squeezing is very high, as squeezing degrades in a highly nonlinear fashion with respect to losses.

STATE RECONSTRUCTION

The state selection protocol enables us to perform a quantum state reconstruction of a selected squeezed state after the noisy channel. Here we can interpret the S_1-S_2 dark plane as the quadrature phase-space as $\langle \hat{S}_3 \rangle \gg 0$.

We select the state with 55.2% transmission. We chose this state because it offers a sufficiently good statistic for all measured angles. We measure the Stokes observables at 30 different angles between the squeezing direction $S_{\theta_{sq}}$ and the anti-squeezing direction $S_{\theta_{sq}+90°}$. At each angle we use a total of $3.15 \cdot 10^6$ samples which are subsequently sorted into 251 bins to derive the corresponding tomograms. Accounting for the anticipated symmetry of the squeezed state we mirror the acquired tomograms to attain a full tomographic dataset of the dark plane. Based on these tomograms, we finally reconstruct the density matrix ρ in the Fock state basis via a maximum likelihood algorithm [30–33]. The reconstruction requires truncating the density matrix to an adequate maximum photon number, where in our case a matrix with dimension 64x64, i.e. with a maximum photon number of 63, proved to be sufficient. Any matrix element of higher order only contributes to the state with a relative weight of less than 10^{-3} with respect to the largest matrix element, i.e. the vacuum state. From the reconstructed state we determine a purity $p = \mathrm{Tr}(\rho^2) = 0.109$. The essential sector of the reconstructed density matrix is plotted in FIG. 5.

A more intuitive grasp of the states properties is provided by means of the Wigner function which we calculate [37] from the reconstructed density matrix. The result is plotted in FIG. 6. In this representation, the comparison between the contour lines of the coherent vacuum state and the reconstructed state directly reveals the preservation of the squeezing.

CONCLUDING REMARKS

We successfully distributed polarization squeezed states through a free-space channel. To the best of our knowledge we show the first distribution of continuous variable non-classical states through the turbulent atmo-

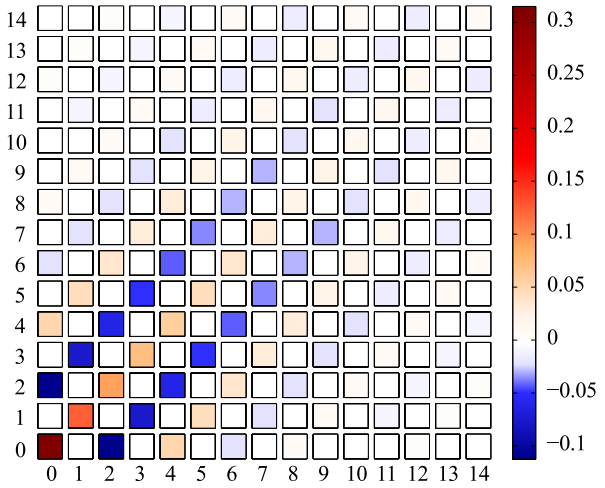

FIG. 5. Top view of the reconstructed density matrix. The integers on the axes refer to photon number states.

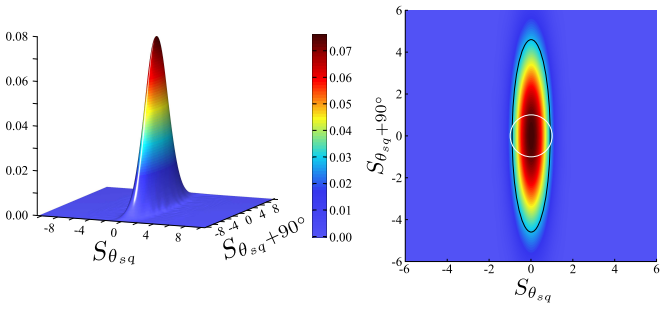

FIG. 6. The reconstructed Wigner-function of a squeezed state after its transmission through the atmospheric free-space channel. On the left hand side we show the three dimensional surface of the Wigner function. On the right hand side the same Wigner function is viewed from the top two dimensionally. The black and white lines visualize the 1/e contour for the squeezed state and the vacuum state respectively.

sphere. We presented a technique for taking into account a natural drifting shot noise variance. Furthermore, we enhanced the amount of squeezing of the state via a state selective protocol and reconstructed a selected state. This substantiates the feasibility of CV free-space quantum communication and paves the way for further free-space quantum communication experiments such as squeezing distillation [38], CV entanglement distribution and distillation [39], or exploiting CV quantum states for atmospheric sensing.

The project was supported under FP7 FET Proactive by the integrated project Q-Essence and CHIST-ERA (Hipercom). The authors acknowledge support of the Erlangen Graduate School in Advanced Optical Technologies (SAOT) by the German Research Foundation (DFG) in the framework of the German excellence initiative.

The authors thank Christoffer Wittmann for fruitful discussions and our colleagues at the FAU computer science building for their kind support and for hosting the receiver station.

* contributed equally to this work
correspondance to: christian.peuntinger@mpl.mpg.de, christoph.marquardt@mpl.mpg.de

[1] R. Ursin, S. Backus, H. C. K. F. Tiefenbacher, T. Schmitt-Maderbach, H. Weier, T. Scheidl, M. Lindenthal, B. Blauensteiner, T. Jennewein, J. Perdigues, P. Trojek *et al.*, Nat. Phys. **3**, 481 (2007)

[2] W.T. Buttler, R. J. Hughes, S. K. Lamoreaux, G. L. Morgan, J. E. Nordholt, and C. G. Peterson, Phys. Rev. Lett. **84**, 5652 (2000)

[3] R. J. Hughes, J. E. Nordholt, D. Derkacs, and C. G. Peterson, New J. Phys. **4**, 43 (2002)

[4] T. Schmitt-Manderbach, H. Weier, M. Fürst, R. Ursin, F. Tiefenbacher, T. Scheidl, J. Perdigues, Z. Sodnik, C. Kurtsiefer, J. G. Rarity, A. Zeilinger, and H. Weinfurter, Phys. Rev. Lett. **98**, 010504 (2007)

[5] A. Fedrizzi, R. Ursin, T. Herbst, M. Nespoli, R. Prevedel, T. Scheidl, F. Tiefenbacher, T. Jennewein, and A. Zeilinger, Nat. Phys. **5**, 389 (2009)

[6] J. Yin, J.-G. Ren, H. Lu, Y. Cao, Y.-P. Wu, C. Liu, S.-K. Liao, F. Zhou, Y. Jiang, X.-D. Cai, P. Xu *et al.*, Nature. **488**, 185 (2012)

[7] S. Nauerth, F. Moll, M. Rau, C. Fuchs, J. Horwath, S. Frick, and H. Weinfurter, Nat. Photon. **7**, 382 (2013)

[8] J. G. Rarity, P. R. Tapster, P. M. Gorman, and P. Knight, New J. Phys. **4**, 82 (2002)

[9] M. Aspelmeyer, T. Jennewein, M. Pfennigbauer, W. Leeb, and A. Zeilinger, IEEE J. Sel. Top. Quantum Electron. **9**, 1541 (2003)

[10] P. Villoresi, T. Jennewein, F. Tamburini, M. Aspelmeyer, C. Bonato, R. Ursin, C. Pernechele, V. Luceri, G. Bianco, A. Zeilinger, and C. Barbieri, New J. Phys. **10**, 033038 (2008)

[11] J. M. P. Armengol, B. Furch, C. Jacinto de Matos, O. Minster, L. Cacciapuoti, M. Pfennigbauer, M. Aspelmeyer, T. Jennewein, R. Ursin, T. Schmitt-Manderbach, G. Baister *et al.* Acta Astronaut. **63**, 165 (2008)

[12] C. Bonato, A. Tomaello, V. Da Deppo, G. Naletto, and P. Villoresi, New J. Phys. **11**, 045017 (2009)

[13] E. Meyer-Scott, Z. Yan, A. MacDonald, J.-P. Bourgoin, H. Hübel, and T. Jennewein, Phys. Rev. A **84**, 062326 (2011)

[14] J.-P. Bourgoin, E. Meyer-Scott, B. L. Higgins, B. Helou, C. Erven, H. Hübel, B. Kumar, D. Hudson, I. D'Souza, R. Girard, R. Laflamme, and T. Jennewein, New J. Phys. **15**, 023006 (2013)

[15] A. A. Semenov, and W. Vogel, Phys. Rev. A **80**, 021802 (2009)

[16] C. Erven, B. Heim, E. Meyer-Scott, J. P. Bourgoin, R. Laflamme, G. Weihs, and T. Jennewein, New J. Phys. **14**, 123018 (2012)

[17] I. Capraro, A. Tomaello, A. Dall'Arche, F. Gerlin, R. Ursin, G. Vallone, and P. Villoresi, Phys. Rev. Lett. **109**, 200502 (2012)

[18] A. Tunick, T. Moore, K. Deacon, and R. Meyers, Proc.

SPIE **7815**, 781512 (2010)
[19] D. Elser, T. Bartley, B. Heim, C. Wittmann, D. Sych, and G. Leuchs, New J. Phys. **11**, 045014 (2009)
[20] B. Heim, D. Elser, T. Bartley, M. Sabuncu, C. Wittmann, D. Sych, Ch. Marquardt, and G. Leuchs, Appl. Phys. B **98** 635 (2010)
[21] V. C. Usenko, B. Heim, C. Peuntinger, C. Wittmann, C. Marquardt, G. Leuchs, and R. Filip, New J. Phys. **14**, 093048 (2012)
[22] M. Hillery, Phys. Rev. A **61**, 022309 (2000)
[23] S. Lorenz, C. Silberhorn, N. Korolkova, R. S. Windeler, and G. Leuchs, Appl. Phys. B **73**, 855 (2001)
[24] V. C. Usenko and R. Filip, New J. Phys. **13**, 113007 (2011)
[25] C Eichler, D. Bozyigit, C. Lang, M. Baur, L. Steffen, J. M. Fink, S. Filipp, and A. Wallraff, Phys. Rev. Lett. **107**, 113601 (2011)
[26] D. A. Lidar, and K. B. Whaley, *Irreversible Quantum Dynamics* 83 (Springer Lecture Notes in Physics, Berlin, arXiv:quant-ph/0301032, 2003)
[27] G. Leuchs, R. Dong, and D. Sych, New J. Phys. **11**, 113040 (2009)
[28] J. Heersink, Dr. rer. nat. thesis, Friedrich-Alexander-Universität Erlangen-Nürnberg, 2006
[29] N. Korolkova, G. Leuchs, R. Loudon, T. C. Ralph, and C. Silberhorn, Phys. Rev. A **65**, 052306 (2002)
[30] Y. Vardi, and D. Lee, J. R. Stat. Soc. B **55**, 569 (1993)
[31] Z. Hradil, Phys. Rev. A **55**, R1561 (1997)
[32] A. I. Lvovsky, J. Opt. B **6**, 556 (2004)
[33] C. R. Müller, B. Stoklasa, C. Peuntinger, C. Gabriel, J. Řeháček, Z. Hradil, A. B. Klimov, G. Leuchs, Ch. Marquardt, and L. L. Sánchez-Soto, New J. Phys. **14** 085002 (2012)
[34] J. Heersink, V. Josse, G. Leuchs, and U. L. Andersen, Opt. Lett. **30**, 1192 (2005)
[35] J. Milanovic, J. Heersink, Ch. Marquardt, A. Huck, U. L. Andersen, and G. Leuchs, Laser Phys. **17**, 559 (2007)
[36] H. A. Bachor, and T. C. Ralph, *A Guide to Experiments in Quantum Optics*, 258 (WILEY, Weinheim, 2004)
[37] J. R. Johansson, P. D. Nation, and F. Nori, Comp. Phys. Comm. **184**, 1234 (2013)
[38] J. Heersink, Ch. Marquardt, R. Dong, R. Filip, S. Lorenz, G. Leuchs, and U. L. Andersen, Phys. Rev. Lett. **96**, 253601 (2006)
[39] R. Dong, M. Lassen, J. Heersink, Ch. Marquardt, R. Filip, G. Leuchs, and U. L. Andersen, Phys. Rev. A **82**, 012312 (2010)